1.C Neutron Streak- and Framing-Camera Diagnostics for ICF Implosions

High-fidelity, time-resolved measurements of the neutron flux from the implosion of DT- and/or DD-filled capsules have been a challenging problem for the international inertial-confinement-fusion (ICF) community. A measure of the neutron production rate can provide valuable information on the quality of the implosion, such as the confinement time of the plasma. A time-resolving neutron detector is generally used to measure the neutron-production rate since the neutron is the fusion product most likely to escape the burn region and the target without further interaction, thus preserving temporal information. The neutron energies are 14.1 MeV and 2.45 MeV for DT and DD fusion reactions, respectively, and typical fusion burnwidths are in the range of 100–300 ps. In this article we report on a new streak-camera diagnostic for directly time-resolving the neutron burnwidth for ICF implosions. The technique uses elastic scattering of the neutrons in CH_2 to convert the neutron signal to a recoil-proton signal, which is proximity coupled to a CsI secondary electron emitter and is subsequently recorded with a standard LLE large-format, x-ray streak camera. Baseline requirements for the neutron detector include the following: directly measured time resolution better than 20 ps; should be positionable to less than 5 cm from the capsule to minimize the transit time spread caused by the velocity distribution of the neutrons (this depends on the neutron source temperature); incorporate an optical or x-ray timing fiducial to establish burn time to within ±20 ps; should be capable of recording on the same shot the time histories of both the primary DD and the secondary DT neutrons (the secondary/primary yield ratio is typically 1%). Further, the instrument needs to be shielded from the background of γ rays, and thermalized and inelastically scattered neutrons originating from nearby diagnostics and the target chamber itself.

Three independent techniques have been used to measure the neutron burnwidth. The first is a neutron streak camera incorporating a UO_2 photocathode.[1–6] U^{238} has a fission cross-section of 1.1 b for 14.I-MeV neutrons, which is equivalent to a 1/e absorption length of 37 cm in UO_2. The cross section for 2.45-MeV neutrons is 0.55 b. The basis of this technique is the large number (>300) of secondary electrons generated in the UO_2 layer by the fission fragments.[7] These secondary electrons have an energy <20 eV and an energy spread FWHM <6 eV, which makes their detection amenable to standard streak-tube electron optics with a time resolution better than 20 ps. However, UO_2 photocathodes suffer from a lack of sensitivity. The photocathode thickness is typically 1–3 μm because of the small range of the fission fragments (<10 μm); therefore, the number of fission events/neutron is $<10^{-5}$. This has led to the proposal and/or development of some complex, large-area photocathode, streak-tube designs that can be positioned close to the neutron source.[1,2,6] These designs can be inefficient (by filtering for a narrow electron-energy spectrum) in collecting the numerous secondary electrons emitted from the UO_2 photocathode, as typically only a few electrons need to be recorded to unambiguously detect an event above the background. Recording 50–100 electrons per fission event only

serves to limit the dynamic range of the streak tube and does not enhance the sensitivity of the detector. Of relevance to this article is the improvement in the secondary electron spectrum when the UO_2 was overcoated with a thin layer of CsI.[6]

A second method for recording fusion burnwidths is to use a neutron-damaged GaAs photoconductor.[8] These small detectors trade off size and therefore sensitivity (active volume to absorb neutrons) for better time response. GaAs detectors ($1 \times 1 \times 3$ mm in size) mounted in a 50-Ω transmission line have demonstrated an impulse response of 60-ps FWHM, but when coupled to a 6-GHz oscilloscope, the time resolution degraded to 130 ps.

The third technique for measuring the neutron flux is to couple the output from a fast scintillator or other neutron-to-light converter to an optical streak camera. This type of detector is currently being used on the GEKKO XII laser facility at Osaka[9] and also on the NOVA laser facility at LLNL.[10] Advantages of these detectors are (1) the small size of the light converter allows it to be positioned <1 cm from the fusion capsule and (2) the streak camera can be placed at a distance from the neutron source where it can be effectively shielded from the radiation background. Coupling to the streak camera is via an optical-fiber bundle or an optical-telescope relay system. The main drawback for the technique is that the impulse response of the converter (which may not be accurately known) must be deconvolved from the signal. Time resolution appears to be limited to about 50 ps.

In this article we present a fourth method for measuring the neutron flux from ICF capsules. Our detector is a standard large-format, LLE x-ray streak tube with a photocathode consisting of a 2500-Å layer of CsI on a 12.7-μm Be foil, which is backed with a 1-mm-thick piece of polyethylene (CH_2, density 0.91 g/cm^3). With this streak camera we have successfully recorded the neutron flux from the implosion of a DT-filled glass microballoon yielding 3×10^{10} neutrons, at a photocathode-to-target distance of 30 cm (Fig. 53.14). The basis of this technique is the generation of recoil protons by elastic scattering of the neutrons in CH_2. Cross sections in hydrogen are 0.7 b for DT neutrons at 14.1 MeV and 2.6 b for DD neutrons at 2.45 MeV, which are equivalent to neutron l/e absorption lengths in CH_2 of 18.3 cm and 4.9 cm, respectively. The recoil protons are forward directed and upon traversing the CsI will lose some of their energy to the electrons in the solid, which in turn generate low-energy secondary electrons. The energy spectrum of the secondary electrons is a characteristic of the photocathode material and not of the energy nor type of the primary excitation source. Therefore, the streak tube operation is identical to that for recording x-ray signals. The Be foil is simply a conductive substrate for the CsI layer, and a different metal foil may be used to moderate or filter the proton energy spectrum.

In the remaining sections of this article we present calculations of the impulse response of the neutron streak camera, followed by a discussion of the experimental results. Finally, we describe a proposal to apply the recoil-proton, radiator photocathode technique to the high-speed framing cameras described in the previous articles.

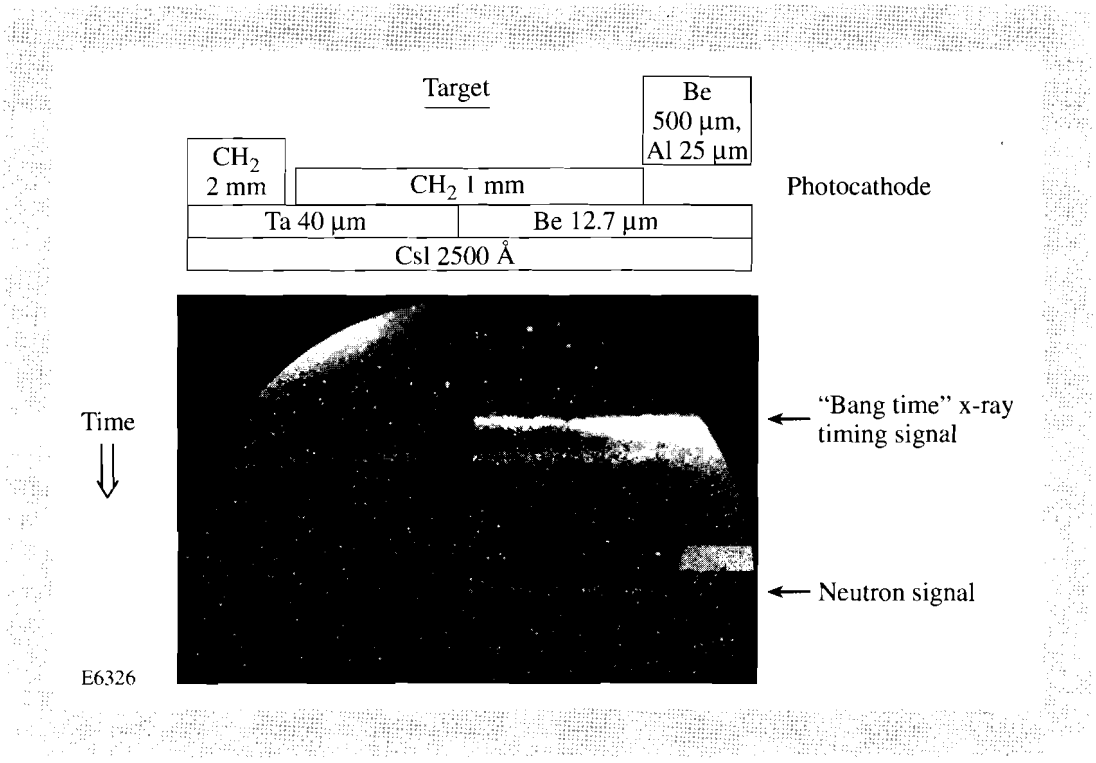

Fig. 53.14
Neutron streak-camera recording of the x-ray and 14.1-MeV neutron signals from the implosion of a DT-filled glass microballoon. Photocathode-to-target distance was 30 cm and the yield was 4×10^{10}. The structure of the photocathode is also detailed. The small rectangle on the right-hand side is caused by x rays transmitted through the photocathode and the anode aperture and recorded directly on the streak-tube phosphor. The source of the signal immediately following the x-ray timing fiducial is unknown at this time.

Photocathode Response

In the limit that the ratio of the neutron absorption length to CH_2 layer thickness is large, the production rate of the recoil protons by neutron-elastic scattering will follow the neutron pulse shape. Therefore, the impulse response of the neutron streak-camera photocathode can be estimated by considering the elastic scattering as a simple binary collision and following the trajectories of the recoil protons, integrating over energy, direction, and initial position. The energy-angle dependence of the protons is given by the formula

$$E_p(\theta) = E_n \cos^2(\theta),$$

where E_p is the proton energy, E_n is the neutron energy, and θ is measured from the forward direction. The recoil protons (whose energies range from zero to the incident neutron energy) are not time resolved and recorded directly by the streak tube; instead, the recorded signal is produced by the low-energy secondary electrons generated by the energy loss of the protons in the thin CsI layer.

Proton-energy loss data as a function of proton energy can be obtained for most materials by interpolation in readily available tables of *dE/dx* values.[11] Given the proton energy-loss curves for the relevant materials, it is straightforward to numerically integrate the proton equation of motion and calculate the time, energy, position, and velocity of the recoil protons as they exit a slab of material. We assume simple nonrelativistic ballistics for the proton and do not include any secondary processes that may introduce straggling, a broadening in the angular and energy distributions. Neither subsequent interactions of the scattered neutrons nor proton-induced x-ray emission is included.

The neutron-sensitive photocathode response is determined from a histogram (by number and/or energy deposited) of the time and spatial position of the energy loss of the recoil protons in a 1000-Å-CsI layer. The initial proton-energy spectrum is flat. The protons are produced uniformly throughout a 1.0-mm-wide slab of CH_2 whose thickness is less than or equal to the maximum proton range, 3.0 mm and 122 μm for 14.1-MeV and 2.45-MeV protons, respectively. Only those proton trajectories that intersect the 1.0-mm-wide photocathode slit are counted. The proton time-of-flight is corrected for the neutron time-of-flight from the initial position of the recoil proton to the CsI layer. The impulse response and the point-spread function (PSF) of the photocathode weighted by energy deposited are presented in Fig. 53.15, for a range of CH_2 thicknesses over a 12.7-μm-thick Be substrate. Since the distribution of energy deposited per proton is fairly narrow (for detecting either DD or DT neutrons), the response calculated by number of events detected is essentially identical to that presented in Fig. 53.15. This implies that the secondary-electron current is linearly proportional to the neutron production rate.

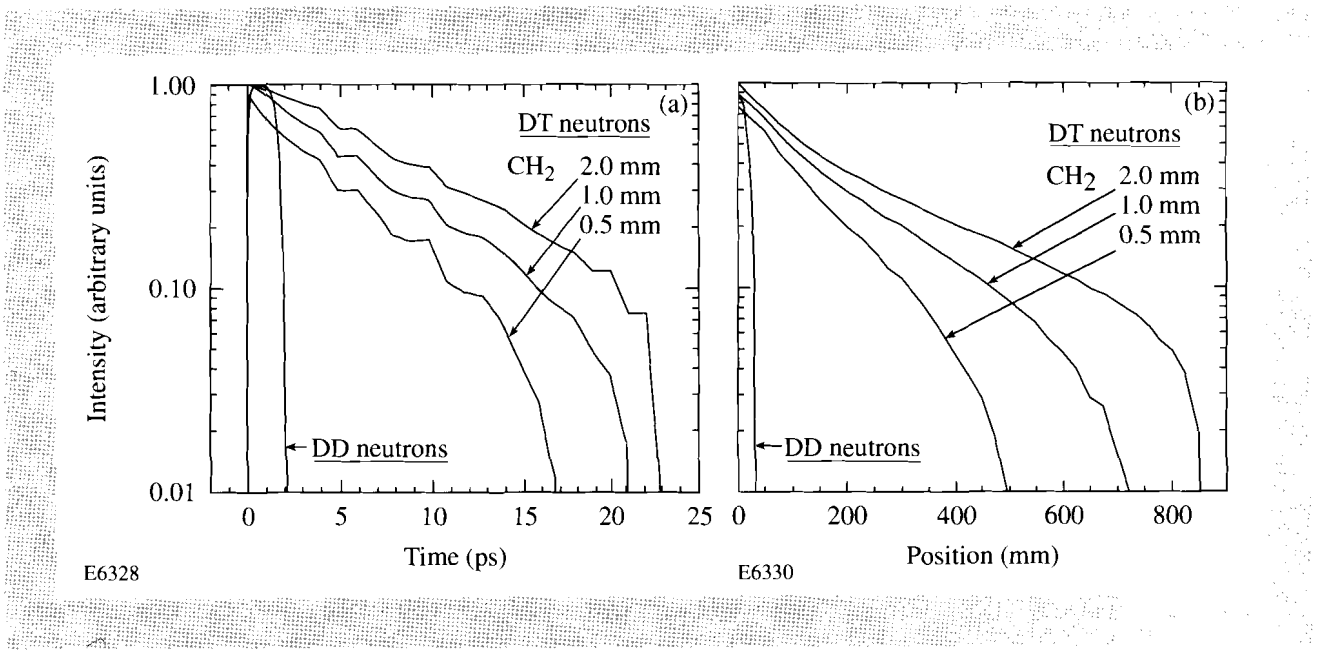

Fig. 53.15
(a) Temporal response of the neutron streak-camera photocathode to an impulse of 14.1-MeV and 2.45-MeV neutrons. The photocathode consists of a 1000-Å-CsI layer on a 12.7-μm-Be foil, which is backed with a 122-μm-CH_2 layer for the DD neutrons and 0.5 mm, 1.0 mm, and 2.0 mm of CH_2 for the DT neutrons. (b) Point-spread function for the same photocathode.

The temporal response to the DD neutrons is less than 2 ps and the maximum extent of the PSF is 30 μm. Nineteen percent of the protons produced in the 122-μm-thick CH_2 layer are detected in the CsI layer. The average energy of the protons entering the CsI layer is 1.0 MeV, and the average energy deposited per proton is 5.0 keV. The DT neutron response varies as expected with increasing CH_2 thickness; the sections nearest the Be/CsI layers contribute most efficiently. The overall detection efficiency of the protons produced in the CH_2 layer drops from 58% to 46% to 31% as the layer thickness increases from 0.5 mm to 1.0 mm to 2.0 mm. The temporal response increases marginally to 23 ps with CH_2 layer thickness, as does the maximum extent of the PSF to 850 μm. The average energy of the protons entering the CsI layer is 8.0 MeV, and the average energy deposited per proton is 1.75 keV. The response of the photo-

cathode to 14.1 MeV neutrons can be improved by replacing the 12.7-μm-Be substrate with a 100-μm-thick Au layer to moderate the protons. Temporal response is reduced to 10 ps and the extent of the PSF to 550 μm; however, the sensitivity also decreases by a factor of 2. We quote maximum values for the responses to hedge for the contribution of straggling effects, which are significant for large energy loss and/or low proton energy at the range limit.[12] These effects will be worse for detecting DT neutrons than for DD neutrons as the recoil-proton range is much larger. Simple estimates for the magnitude of the effect of straggling may be obtained by artificially modifying the energy loss in the CH_2 as the proton slows down. Low-energy stragglers are created by increasing the dE/dx values. This decreases the proton range and actually improves the photocathode response. High-energy stragglers have a longer range in the CH_2 and can double the temporal response and the PSF for a 2.0-mm-thick CH_2 layer; the responses with a 0.5-mm-thick CH_2 layer are degraded by about 50%. Replacing the Be substrate with a 100-μm-Au foil reduces the effects of straggling in the CH_2 layer to negligible magnitudes. For a DD neutron detector the degradation of the temporal response by energy straggling will not be worse than 8 ps—the stopping time for a 2.45-MeV proton in CH_2.

A simple estimate for the quantum efficiency of the CsI layer to the recoil protons can be made as follows. It has been shown experimentally that for protons (with energies ranging from 10 keV to tens of MeV) bombarding thin metal foils, the secondary-electron yield is proportional to the electronic stopping power within an accuracy of 10%.[13] dE/dx includes all the processes that contribute to the energy transferred to the electrons in the solid, which then cascades into secondary electrons. The forward-surface, secondary-electron yield for metals (Y_f) is approximately

$$Y_f = 0.017\, dE/dx,$$

where dE/dx is measured in keV/μm. The secondary-electron yield for proton bombardment of insulators is about ten times higher than for metals.[14] This can be understood because the secondary-electron mean-free paths are larger in insulators than in metals. Using the tabulated values of dE/dx to calculate the proton energy loss and a factor of 30 for the ratio of the secondary-electron yields for CsI to Au (as measured for x rays in the few-keV region[15]), we estimate that the number of secondary electrons emitted per event is 5–10 for DT neutrons and 15–25 for DD neutrons. The overall detection efficiency for DT neutrons is about a factor of 8 higher than for DD neutrons, mainly because of the larger ratio of the recoil-proton range to neutron cross section.

Experimental Results

The direct-drive target implosions were carried out using the 24-UV-beam OMEGA laser system. Typical parameters for the series of high-yield target experiments were 850 J to 1350 J in a 600-ps-FWHM Gaussian pulse delivered to a 320-μm-diam, 1.1-μm wall-thickness target filled with a 10-atm equimolar mixture of DT gas. These experiments produced 14.1-MeV neutron yields in the range of 3×10^{10} to 1×10^{11}. A few DD gas-filled targets were also imploded but the highest DD neutron yield for this series was 10^9 and no signal was observed.

Experimental results including the details of the neutron streak-camera photocathode are presented in Fig. 53.14. The streak record shows the bang-time x-ray emission followed 4.9 ns later by the DT neutron-generated recoil-proton signal. The neutron signal is clearly observable above the background level, which consists of some very bright speckles superimposed on a fairly uniform pedestal, outlined by the edge of the 40-mm-diam microchannel-plate (MCP) image intensifier. The neutron signal through the Be substrate is marginally brighter than through the Ta substrate; calculations predict a difference of 16%. Similarly, the section with 2.0 mm of CH_2 is predicted to be 37% brighter than the section with the 1.0-mm thickness. The streak speed for these preliminary experiments was 430 ps/mm at the output screen, to allow recording of a signal from the slower DD neutrons (13 ns after the x-ray signal). Although the slow streak speed severely limits the time resolution for the streak camera, there is a weak indication that the neutron signal recorded through the Ta substrate is slightly shorter than through the Be foil. A lineout through the reduced data is presented in Fig. 53.16. The high-energy, x-ray signal (filtered for E > 6 keV) is narrower than the 175-ps-FWHM neutron signal. The source of the emission peak 1 ns after the x-ray signal is unknown at this time. It is also present for non-neutron target shots and could perhaps be caused by x-ray fluorescence from plasma blow-off hitting the nose cone of the instrument.

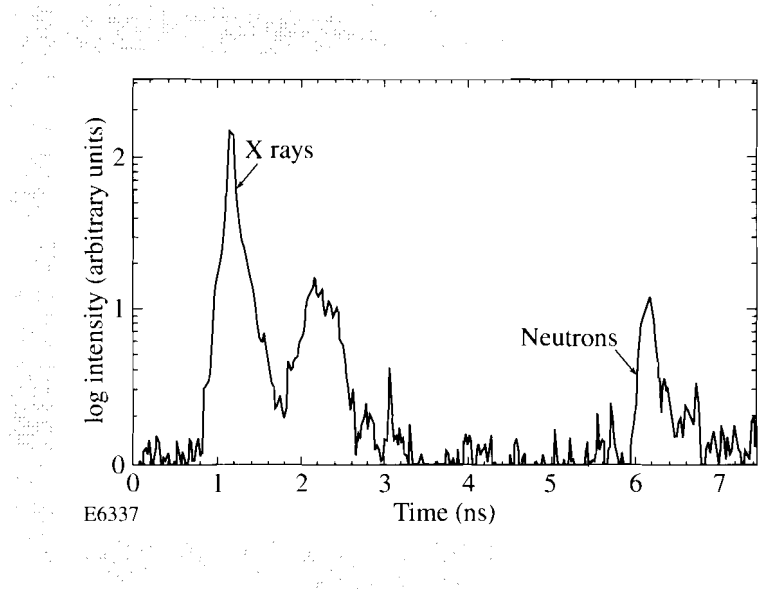

Fig. 53.16
Lineout of the x-ray bang-time signal followed 4.9 ns later by the neutron-generated signal. The source of the peak at $t = 2.5$ ns is unknown at this time.

The speckle noise in the recorded streak data is indicative of channel saturation in the MCP. Whether this is because of neutrons or γ rays interacting with the MCP itself, or with the streak-tube phosphor screen, and when it occurs (ns or μs after the implosion) needs to be investigated further. Similarly, the cause of the broad pedestal on the streak records needs to be resolved. Since the speckle is always positive valued, it can be easily removed. We use an algorithm that takes line segments in the spatial direction, calculates the average and standard deviation σ, and then replaces pixel values that exceed the average by more than 3σ with the average. This technique just clips the peaks and doesn't affect the time resolution of the streak record. Typically, two or three passes across the data

set are sufficient. Median or Fourier transform-filtering techniques would smooth out both the valleys and the peaks and thereby compromise the time histories. The broad pedestal is subtracted from the data after removing the speckle. As the streak camera is moved closer to target, the speckle noise will increase in the same ratio as the neutron signal and remain bothersome. Eventually the speckle and the pedestal will become problematic as they use up the available dynamic range of the recording system. To overcome this we are currently working on a new, small-diameter, large-aspect-ratio, streak-tube design that will allow us to get within 5 cm of a direct-drive target, and allow shielding to be placed between the neutron source and the phosphor/intensifier recording system.

Framing-Camera Neutron Detector

The concept of using a recoil-proton radiator as part of the photocathode in a neutron detector can also be applied to high-speed framing cameras (Fig. 53.17). These cameras use <100-ps duration, kilovolt electric pulses propagating along gold microstrip lines coated onto microchannel plates to generate 37-ps-duration frame times as described in articles 1.A and 1.B of this volume.[16] The CH_2 layer for such a detector would be in contact with the channel plate to minimize any time dispersion introduced by proton time-of-flight across a gap. The recoil proton would generate secondaries in the gold layer, which extends a channel diameter or so down the channel, or in the top surface layers of the channel itself. These secondary electrons are either quickly reabsorbed on the channel walls or, if the electrical pulse is present, accelerated down the channel and amplified. Sensitivity could be enhanced by a coating of CsI on the microstrip line. We don't anticipate any significant degradation of the voltage pulse on the strip line by having the proton radiator in contact.

Although the time resolution of the detector is limited to the frame time, the advantage of using this type of detector is the increased sensitivity available with a larger area sensor. The propagation speed of the electrical pulse down the strip line is 7 mm/35 ps. If the plate is tilted such that the electrical pulse propagation

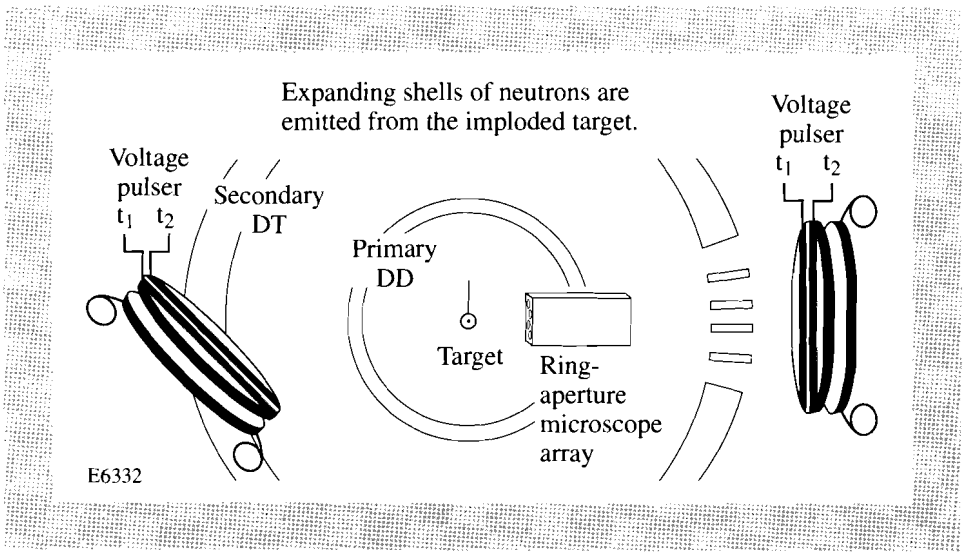

Fig. 53.17
Concept for a neutron-sensitive framing camera as a detector to measure both the primary and secondary burnwidths, or, when coupled to an array of neutron microscopes, to do time-resolved neutron imaging of the core.

direction is at 45° to the neutron velocity vector, the effective area per resolution element is 7 mm * sin 45° * width (7 mm) or 35 mm^2 (see Fig. 53.17). The plate is tilted to simplify synchronization of the gating pulse to the neutron signal; the time window is the length of the projection of the strip onto the neutron velocity vector divided by the neutron speed. At 45°, a 40-mm-long plate has a synchronization window for DT neutrons of 550±200 ps, depending on whether the electrical pulse propagation direction is toward or away from the target. The multiple strips available on the plates can be individually timed to allow overlapping frames or to detect primary- and secondary-neutron signals, which come at different times. With a pair of framing cameras separated by about 30 cm, one can conceive of performing ion-temperature measurements. The Doppler broadening of the DT neutron pulse is given by[17]

$$\Delta t(ps) = 1.2 * d(cm) * \sqrt{T_i(\text{keV})} ,$$

where d is the target-to-detector distance and T_i is the DT ion temperature. One just requires a resolvable broadening of the neutron pulse during the transit time between the pair of detectors. Another intriguing application of this technique is to take advantage of the narrow PSF for detecting DD neutrons and develop a high-speed, multiframe, neutron-imaging detector. The imaging could be accomplished with an array of penumbral-aperture,[18] or ring-aperture microscopes. Time-resolved neutron imaging should be possible for DD neutron yields >10^{12}.

The noise background with the framing-camera detector will potentially be less than for a streak-camera system because the gain element is on for a very short duration. In comparison, streak-camera intensifiers are generally active for 0.5 ms and integrate the long, low-level background signals.

Summary

We have demonstrated a prototype neutron streak camera capable of directly time-resolving the fusion-reaction burnwidth with an estimated time resolution <20 ps for DT neutrons and <10 ps for DD neutrons. The sensitivity of our recoil-proton radiator, close coupled to a CsI secondary-electron emitter, is comparable to detectors, based on coupling the emission from plastic scintillators to optical streak cameras, and orders of magnitude better than UO_2 photocathode-based detectors. The recoil-proton energy loss in the CsI layer follows the neutron production rate directly; there are no long-decay-time fluorescence emissions to deconvolve. Calculations indicate that the detector is about eight times more sensitive for recording DT neutrons than DD neutrons, making it favorable for recording primary- and secondary-neutron burnwidths on the same shot. We have also presented a concept for applying recoil-proton radiator photocathodes to high-speed framing cameras.

ACKNOWLEDGMENT

This work was supported by the U.S. Department of Energy Office of Inertial Confinement Fusion under Cooperative Agreement No. DE-FC03-92SF19460, the University of Rochester, and the New York State Energy Research and Development Authority. The support of DOE does not constitute an endorsement by DOE of the views expressed in this article.